

Synergy of CP-DGPS, Accelerometry and Magnetic Sensors for Precise Trajectory in Ski Racing

Jan Skaloud, Philippe Limpach
Swiss Federal Institute of Technology Lausanne (EPFL)

BIOGRAPHY

Jan Skaloud is a scientist and lecturer at the Institute of Geomatics at EPF Lausanne, Switzerland. He holds a Ph.D. and M.Sc. in Geomatics Engineering from the University of Calgary and Dipl. Ing. in Surveying Engineering from the Czech Institute of Technology, Prague. He has been involved with the GPS research and development since 1993 and has worked extensively on the integration of GPS and inertial navigation systems for precise airborne and terrestrial mapping.

Philippe Limpach is a recent graduate from the Swiss Federal Institute of Technology Lausanne with a M.Sc. degree in Geomatics Engineering.

ABSTRACT

This paper presents the conceptual and technical aspects of a system in development that precisely determines athlete's trajectory through a course. Carrier phase-based (CP-DGPS) positioning represents core of the system, while tri-axial accelerometer and magnetic sensors act as an autonomous aid that offers instantaneous attitude determination and can potentially help when navigating through GPS signal blackout zones. Trajectory representation by a set of continuous functions with geometrical constraints supplies an effective tool that removes outliers and discontinuities in the positioning and offers better base for deriving acceleration profiles. Successfully tested in competitive skiing, the concept is also applicable in other fields for tracking objects on restricted trajectory.

INTRODUCTION

In constant search of improvements, competitive skiing asks not only for exceptional athletes but also for performing positioning [1], [2]. Precision is needed because the differences that distinguish the fastest line from the others are often minute. Currently used performance-evaluating methods rely either on time measurements or on video motion analyses. The timing

data indicates only a summary of good and bad moves over a given section, while the information based on monoscopic imagery is purely qualitative. In open spaces the use of CP-DGPS offers position, velocity and acceleration (PVA) analysis of racers' trajectories with accuracies the coaches never dreamed about. The reality is, however, often far from such an ideal case as the skier's environment is quickly alternating between open spaces and areas that are adverse to the reception of satellite signals. Considering the relatively high dynamics of a skier and the ergonomic requirements placed on the equipment, today's technological limits in positioning are quickly reached if not exceeded. Combining high performance GPS receivers with miniature autonomous navigation aids and appropriate trajectory modeling extends these limits considerably.

The first part of the paper briefly discusses the limits of the state-of-the-art carrier phase GPS positioning in dynamic environments. Then the focus is on trajectory modeling, where positioning improvements are sought by imposing constraints of continuity and smoothness when restituting trajectory from the sparse sampling. This process is governed by smoothing piecewise cubic splines and has several advantages over other possible interpolants as it provides an effective and realistic filtering across all PVA components. The result is continuous motion functions that permit direct computation of the kinematics acceleration. Further we discuss the merge of GPS-obtained acceleration profile with the 3D-digital compass data (i.e. the magnetic field and the specific force) to derive instantaneous 3D attitude. Numerical examples and tests are given in each particular section. In most cases the data come from training session of the men's and women's downhill during the Ski World Championship in St. Moritz, 2003.

CP-DGPS POSITIONING UNDER LESS FAVORABLE SATELLITE SIGNAL RECEPTION

In competitive skiing, the separation between the reference and the rover receivers remains below 5 km. This puts the ambiguity determination process to the category of short-baselines where simple models apply

and the algorithm theory expects little problems when using given set of dual frequency measurements [3]. The quality of phase measurements remains, however, hardware-dependent and such reliance becomes more profound when the conditions of satellite signal reception changes quickly, sometimes abruptly. The factors of most importance are:

- Phase-measurement accuracy under low SNR and high acceleration.
- Speed of signal reacquisition after partial and complete loss-of-lock.
- Speed of L2 acquisitions and tracking accuracy.

As the manufacturer specifications are sometimes deceptive in these aspects, we conducted a practical testing with several high-end dual frequency receivers operating under dynamic conditions that generated frequent partial or complete loss-of-lock. The RF signal was split between the contenders and a precise GPS/INS integrated system was used to provide the reference for the performance evaluation.

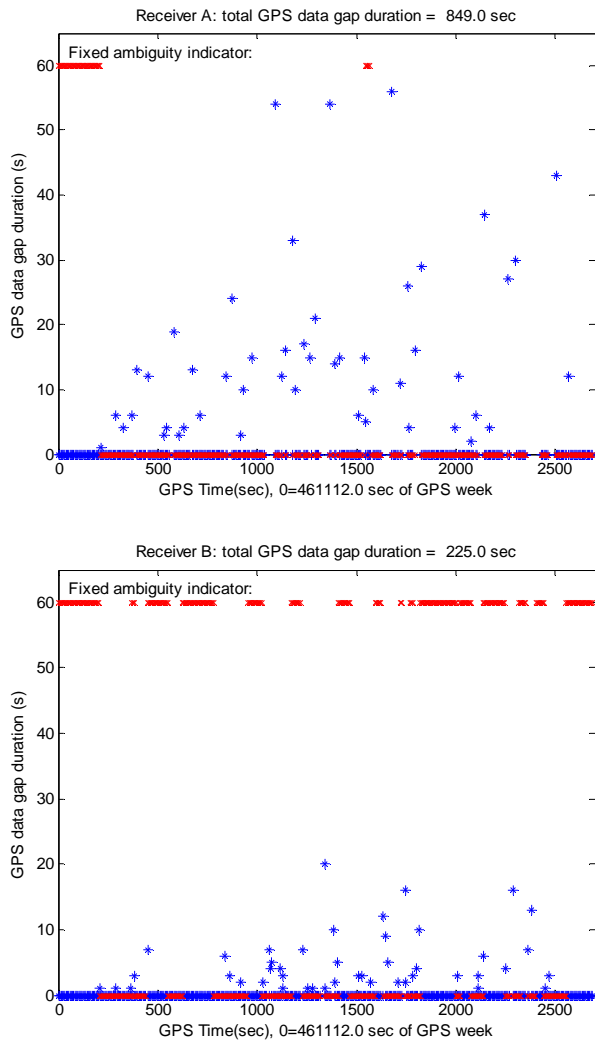


Figure 1: Influence of the hardware choice on signal tracking and ambiguity resolution: comparison between 2 high-end receivers.

We do not aim to present here comprehensive studies in these aspects but rather demonstrate that the hardware differences under such conditions are much more decisive for precise positioning than the existing nuances between the latest developments in ambiguity resolution algorithms. Figure 1 demonstrates this by displaying comparison of signal tracking periods (4SV) and the corresponding ambiguity success rate for two simultaneously employed receivers. As can be seen from this comparison, considerable differences were revealed in terms of the speed of signal acquisition and tracking that influence the success rate of ambiguity fixing.

Finding the correct set of ambiguities enables the sub-decimeter or even cm-level positioning and most of the trajectory related information could be derived based upon this information. Nevertheless, the quick alternation of good and less favorable satellite signal tracking conditions due to changing environment (typical for ski-racing as well as many other terrestrial-kinematic applications of GPS) results in varying positioning accuracies and irregular trajectory sampling. Autonomous sensors could be theoretically employed to provide the necessary data-gap bridging and smoothing tool. Before looking at this possibility we will, however, investigate to which extent such a role could be attributed to the method of trajectory interpolation and modeling.

TRAJECTORY MODELING AND REPRESENTATION

Curve representation in 3D

Representing a trajectory by mathematical function rather than by a set of discrete points creates a base that is not only better suited for subsequent analysis (deriving curvilinear distance, curvature, acceleration, etc.) but can – to some extent - participate in data filtering. This is especially the case when some external assumptions can be made about some trajectory parameters.

Following [4], a curve in \mathbf{R}^3 (3D space) is a differentiable function $c: I \rightarrow \mathbf{R}^3$, from an open interval I in the real line \mathbf{R} , if c is a continuous and differentiable vector-function, defined by:

$$c(t) = (x(t), y(t), z(t)) \quad \forall t \in I \quad (1)$$

where $x(t)$, $y(t)$, $z(t)$, are its Euclidean coordinate functions. One can picture a curve in \mathbf{R}^3 as a trip taken by a moving point c . At each "time" t in some open interval, c is located at the point $c(t) = (x(t), y(t), z(t))$ in \mathbf{R}^3 .

Choice of interpolation function

In order to obtain continuous mathematical functions in \mathbf{R}^3 we have to model the trajectory by interpolation functions, where the discrete positions measured by GPS operate as adjustment points. For various reasons stated later, the chosen interpolant will be based on cubic

splines. This represents a piecewise interpolation by cubic polynomials between adjustment points. Being a piecewise interpolation, cubic splines take in account different trajectory behavior at each interval, but they also respect continuity conditions with regards to position, velocity and acceleration at each adjustment point. It can be shown that cubic splines minimize, among all interpolation functions, acceleration on the curve, which well corresponds to the physics of skier's motion. Further, we will see that some form of filtering can be relatively easily achieved when considering smoothing splines. When considering these properties we can state that cubic splines are well suited for trajectory modeling and interpolation in downhill skiing.

Definition of cubic splines

The theory of splines is fairly well-known and well documented in the literature [5], [6], hence we limit ourselves only to a brief description needed in subsequent sections.

Let $a = t_0 < t_1 < \dots < t_n = b$ be points dividing the interval $I = [a, b]$ in the union of intervals $I_k = [t_k, t_{k+1}]$. The couples $(t_k, f(t_k))$, where $k = 0:n$, are the $n+1$ adjustment points for interpolation.

A cubic spline, interpolating f , is the interpolation function S that satisfies the following conditions:

1. On each interval $I_k = [t_k, t_{k+1}]$, with $k \in [0 .. n-1]$, S_k is a cubic polynomial with coefficients c_{ki} , i.e.

$$S_k(t) = \sum_{i=1}^4 (t-t_k)^{4-i} c_{ki} \quad (2)$$

2. $S(t_k) = f(t_k)$ for $k \in [0 .. n]$

As there are $n + 1$ adjustment points, there will be n intervals and also n cubic polynomials. These n cubics have $4n$ degrees of freedoms, which are the 4 coefficients of each cubic.

$4n - 2$ degrees of freedom can be defined by the following conditions with $S_-(t_k)$ and $S_+(t_k)$ denoting the left-hand and right-hand limits of S at t_k :

$$\begin{aligned} S_-(t_k) &= f(t_k), & \forall 1 \leq k \leq n-1, \\ S_+(t_k) &= f(t_k), & \forall 1 \leq k \leq n-1, \\ S(t_0) &= f(t_0), \\ S(t_n) &= f(t_n), \\ S'_-(t_k) &= S'_+(t_k), & \forall 1 \leq k \leq n-1, \\ S''_-(t_k) &= S''_+(t_k), & \forall 1 \leq k \leq n-1, \end{aligned} \quad (3)$$

The relations (3) yield $2(n-1)+2+2(n-1) = 4n-2$ conditions. Hence, two more conditions are necessary in order to specify the problem completely. Common choices for these last conditions, called end conditions, are

$$\begin{aligned} S'_+(t_0) &= 0 & \text{and} & & S''_-(t_n) &= 0 \\ S'_+(t_0) &= p_0 & \text{and} & & S''_-(t_n) &= p_n \end{aligned} \quad (4)$$

If the first condition is used, then the solution to the interpolation problem is referred to as the natural cubic spline. Generally, it is recommended to apply the second condition [5], where the needed estimate of the slope can be calculated from the data.

In the interpolation problem of 3D trajectories, we have to determine one cubic spline for each of the 3 coordinates (X, Y, Z), in order to obtain the 3 Euclidean coordinate functions $x(t), y(t), z(t)$ of (1). Hence, on each coordinate axis we have separate cubic polynomials for each interval that are delimited by two succeeding adjustment points. The variable t of (1)-(4) will thus represent the GPS time.

Application to downhill skiing

To demonstrate the suitability of cubic splines for trajectory modeling in alpine skiing, we investigate the necessary sampling rate that guarantees small interpolation error. We chose a GPS trajectory of good measurement quality and uninterrupted signal tracking acquired during downhill course of the World Ski Championships in St. Moritz (Switzerland) in February 2003. Based on the original trajectory measured at 10 Hz, we chose four sets of adjustment points, characterized by different time intervals. Cubic splines are computed for each set of adjustment points, allowing to determine the 'control' curve points at 10 Hz interval by interpolation. In this manner, we can compare the original trajectory coordinates at 10 Hz with the interpolated ones. The statistics of such comparison are summarized in Table 1.

Table 1: Influence of data sampling on interpolation error. (*For characteristic points the results are based on smoothed splines, see the text below for explanation.)

Sampling interval No. of points	2Hz 200	1Hz 100	0.5Hz 50	Char.pts* 90
Mean horizont. Diff (m)	0.02	0.09	0.73	0.30
Horizontal 1σ (m)	0.02	0.09	0.65	0.30
Mean vert. diff (m)	0.03	0.12	0.42	0.17
Vertical 1σ (m)	0.03	0.13	0.38	0.16

We can conclude from this table that the skier's motion can be well approximated by cubic splines ($1\sigma = 0.1\text{m}$) if the measurement frequency is 1 second or higher. In other words, only 10% of the original 10Hz data is needed to model the trajectory. Later, we will take an advantage of this knowledge when filtering the trajectory for sudden jumps due to abrupt change in satellite constellation or quick change in the measurement accuracy (changing float to fix ambiguities or vice versa).

The last column in Table 1 studies the trajectory restitution using characteristic points. In the planar component this set comprises inflection points, points of maximum curvature and gate intersection points, while in the height component we consider only height inflection points and points of maximum height curvature.

The use of characteristic point is motivated by the fact that their spatial location in certain areas varies minimally between skiers and could be possibly detected in time by autonomous sensors (i.e. horizontal inflection points correspond to zero radial accelerations or zero rate in azimuth). We can see from the table that the number of characteristic points used in trajectory reconstruction is almost the same as in the case of 1Hz interpolation, however, with different spatial distribution. The positioning differences with respect to the true trajectory are somewhat larger, however part of it comes from the fitting that is based on smoothing rather than on ‘normal’ splines. Interpolation by smoothing splines does not guarantee exact reproduction of adjustment points and therefore can introduce additional interpolation errors (here in decimeter-range). Therefore, such approach should be used cautiously on data of uniform accuracy. Its greatest strength, however, lies in combination of data points of varying precision, as will be explained in the subsequent section.

TRAJECTORY SMOOTHING

As previously mentioned, smoothing splines can be accommodated for non-exact fits between the adjustment points and thus offer some form of spatial filtering. This property can be used to reduce high frequency noise, bridge over data ‘outliers’ or to provide smooth transitions when sudden position ‘jumps’ due to change in satellite constellation or ambiguity fixing are encountered.

Smoothing cubic splines

The derivation of smoothing splines comes from the variational approach, where cubic splines are obtained as the best interpolant minimizing a quadratic cost function:

$$\sum_{i=1}^n w_i (x_i - S(t_i))^2 + \lambda \int_a^b \left(\frac{\partial^2 S(t)}{\partial t^2} \right)^2 dt \quad (5)$$

for the given data (t_i, x_i) with corresponding weights w_i on an interval $t \in [a .. b]$ and specified smoothing factor $\lambda \in [0 .. 1]$. The first term of (5) represents the error measure due to data fitting proximity, while the integral part symbolizes the roughness measure (smoothness of the trajectory). The art of using the smoothing spline consists in choosing λ and w so that S contains maximum of the information, and minimum of the noise present in the data.

The expectation on certain levels of trajectory ‘smoothness’ varies with the nature of each application and can change between curve sections. When $\lambda=0$, S becomes the straight line fit to the data in the least-square sense, while at other extreme ($\lambda=1$) S takes the form of the ‘natural’ cubic spline interpolant reproducing the input data. In our case of downhill data, satisfactory results were obtained already for non-time varying $\lambda \sim \in [0.5 .. 0.75]$. For courses with more varying curve-shapes we suggest to adapt λ according to the magnitude of error in the second

derivative, providing this could be obtained by some other independent measurements (i.e. from accelerometers). The questions of choosing appropriate weights will be addressed in the following part.

Smoothing trajectories of varying data quality

Sudden drops or re-acquisitions of satellites signals as well as ambiguity fixing cause significant discontinuities in the trajectory shape that do not correspond to the actual movement of a racer. We present here a strategy that tends to diminish such effects and result in more realistic route shapes of higher accuracy.

As the changes in satellite constellation and the float to fixed ambiguity passages are accompanied by the drops/gains in the positioning accuracy, it is quite natural to allow more relaxed fits for data of higher uncertainty while asking for closer approximation when the confidence rises. These fitting differences can be realized in (5) by varying the weights w_i between the adjustment points with respect to the estimated position accuracy. We suggest considering also the fixed/float ambiguity status and determine the i^{th} entry of the weight vector w as

$$w(i) = \frac{w_{amb.status}(i)}{\sigma_{pos}(i)} \quad (6)$$

where, $\sigma_{pos}(i)$ is the position standard deviation in meters and $w_{amb.status}(i)$ is a parameter changing in respect to the fixed/float ambiguity status as shown in Figure 2.

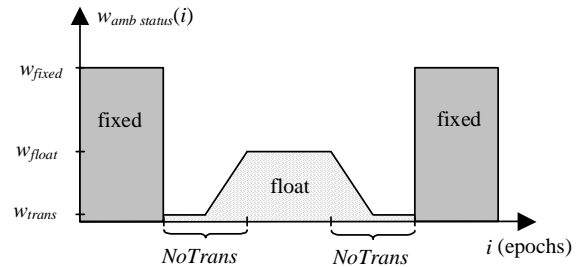


Figure 2: Evolution of the weighting factor $w_{amb.status}$ with respect to the fixed/float ambiguity status.

In the case of fixed ambiguities, $w_{amb.status}(i) = w_{fixed}$ the value of which is normalized to 1. In the case of float ambiguities $w_{amb.status}$ takes different values from the interval $[w_{trans} .. w_{float}]$. A number of transition epochs at the beginning and at the end of a float ambiguity period are defined by the parameter $NoTrans$. Epochs of float ambiguities neighboring the epochs of fixed ambiguity take $w_{amb.status}(i) = w_{trans}$ which is of very low value ($\sim 10E-4$). Such strong de-weighting avoids jumps in the modeled trajectory due to sudden drops of accuracy while relying on the movement prediction due to athlete’s inertia. For other transition epochs, $w_{amb.status}$ is linearly increasing in time from w_{trans} to the final value of w_{float} , which is the value of $w_{amb.status}(i)$ for epochs of float ambiguities outside the transition periods. In our experience we set this value to a half of the w_{fixed} to scale down the rather

optimistic positioning accuracy estimates for these periods. We also recommend to double or triple the weight on the last ‘fixed’ epoch before a ‘float’ period, as well as on the first ‘fixed’ epoch after a ‘float’ period. The high weight value will force the spline to get even closer fit to these adjustment points and reduce the interpolation error for the periods of transition.

Example: Data gaps and phase data of poor accuracy

Two examples are shown to illustrate the benefit of smoothing splines with varying error weights. The first example (Figure 3) represents a real case of bad GPS data period of float ambiguities due to deprived phase data producing jerk in the trajectory followed by few epochs of no positioning solution (complete loss of lock). The smoothing spline with uniform weight distribution (dotted line) results in somewhat smoothed but still apparent jump at the fixed/float transitions, while the smoothing spline with suggested variation of weights (full line) is closer to the real trajectory taken by the skier as verified on the video-footage during his passage of the gate.

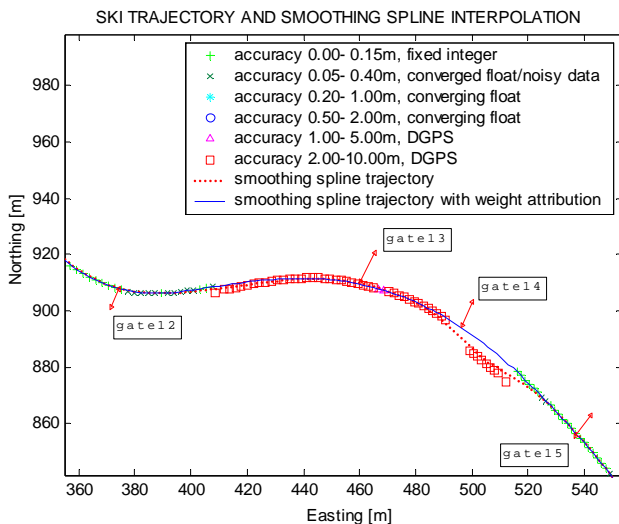


Figure 3: Ski trajectory modeled by smoothing spline. Real case of bad GPS data period with float ambiguities producing a trajectory ‘jump’ followed by some epochs of complete loss of lock (no data). Skier’s head with the GPS antenna attached to his helmet sometimes leaps outside the gate in the effort to steer the skis as close as possible to the inside pole.

Example: Partial satellite blockage

The second example (Figure 4) considers a situation of a sudden partial blockage of satellite signal due to environmental obstructions. Only 4 satellites are visible during several seconds, which corresponds well to circumstances encountered in downhill skiing. This signal masking is produced artificially in post-processing by omitting from the solution a few satellites that are near to horizon. The real trajectory of sub-decimeter accuracy is thus available and serves as a reference (dots). It can be seen from the figure that the ‘normal’ smoothing spline (dashed line) smooths the jump at the fixed/float transitions only partially, while the smoothing spline with different error weights (full line) is close to the real trajectory points.

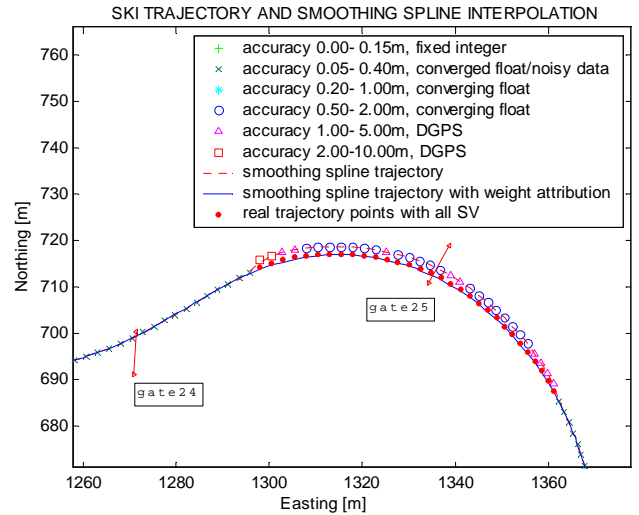


Figure 4: Ski trajectory modeled by smoothing spline: simulated case of 3-second drop-off of low elevation GPS satellites.

ACCELERATION PROFILE BY CP-DGPS

The acceleration profile is of immense interest to coaches as it can serve to identify the committed faults in the skier’s technique and to recognize the performance of the equipment (e.g. waxing, ski manufacturer, etc.).

Since acceleration is not direct GPS observable, it has to be numerically derived from the changes in position or velocities. The numerical post-mission differentiation can also be applied to carrier phase observation to obtain less noisy estimates of its instantaneous derivative. This subsequently leads to more accurate velocity estimation. A number of basic methods have been suggested for this approach spanning from curve fitting, Taylor series approximation [7] to the more rigorous approach of optimal filter design [8] also used in sports applications [2]. Once the trajectory has been modeled as a continuous function, the acceleration can be obtained as its time derivative. Such method may be associated with the category of curve fitting. We will show that in the case of smoothing spline this approach is at least as appropriate for our application as the optimal filter design.

Velocity and acceleration from splines

Let $c: (a, b) \rightarrow \mathbf{R}^3$ be a curve as defined in (1). For each $t \in (a, b)$, the tangent and normal vectors to the curve at t are the vectors

$$\begin{aligned} T(t) &= \dot{c}(t) = (\dot{x}(t), \dot{y}(t), \dot{z}(t)) \\ N(t) &= \dot{T}(t) = \ddot{c}(t) = (\ddot{x}(t), \ddot{y}(t), \ddot{z}(t)) \end{aligned} \quad (7)$$

with the single and double dots denoting the first and second time derivatives, respectively. The $T(t)$ is also called velocity vector and $N(t)$ the acceleration vector. The speed at t is the real number $\|T(t)\| = \|\dot{c}(t)\|$, while

acceleration at t is the real number $\|N(t)\| = \|\ddot{c}(t)\|$. Apart from indicating the instantaneous velocity, the tangent vector can serve in deriving the azimuth of the curve.

The relation (7) is valid for any continuous function that is at least twice differentiable. As this is the case of the cubic spline, the derivation of the acceleration profile is rather straightforward once the piecewise model gets established. Figure 5 compares the spline approach with the ‘optimum filter’ method as studied in [2]. It can be seen that the acceleration derived from smoothed spline follows closely that from an optimal differentiator, although some small local differences are apparent. In the absence of an independent reference it is difficult to provide further conclusions. However, as the spatial filtering precedes the differentiation process, we can state that the proposed approach is most likely less sensitive to jerk effects due to sudden changes in satellite constellation or ambiguity fixing because their influence was already mitigated. Finally, the third curve in Figure 5 highlights the fact that the application of ‘normal’ spline is less appropriate as it yields an estimate that is as noisy as differentiators of low-order Taylor series.

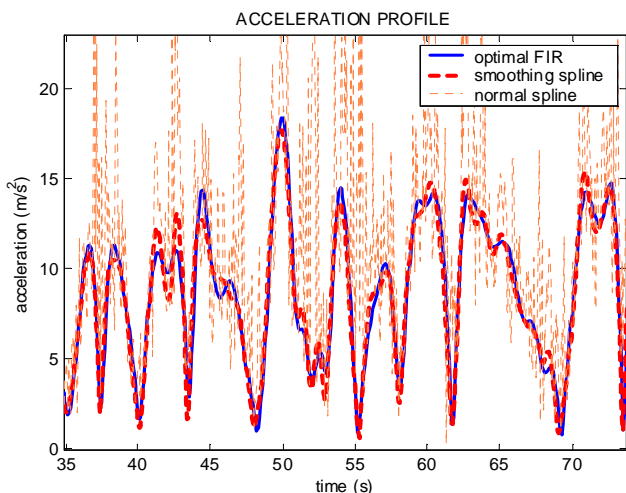


Figure 5: Comparison between different methods for deriving kinematic acceleration from GPS data.

ATTITUDE AND ACCELERATION PROFILE USING MEMS DMC/GPS

We now turn our attention to the sensors from the microelectromechanical (MEMS) family to find an autonomous alternative in deriving the acceleration and investigate the possibility of determining the attitude. For that purpose we shall consider a 3-axis Digital Magnetic Compass (DMC) comprising triaxial magnetometers and accelerometers. For the moment we assume that the 3-axis MEMS gyroscopes are not present, although there is an increasing number of systems combining all these components into augmented inertial measurement units (IMU).

Concept of instantaneous 3D attitude determination via DMC/GPS

This concept of attitude determination exploits the old Wahba’s problem [9] where the orientation of a rigid body (R) is sought based on weighted (p) measurements of unit vectors in two coordinates systems: the body-frame (b) and the system of reference (r).

$$J(q) = \frac{1}{2} \sum_{i=1}^k p_i (b_i - R(q)r_i)^2 \quad (8)$$

When quaternion (q) parametrization of the rotational matrix is used, the attitude can be unambiguously found when minimizing the relation (8) with a condition $q^T q = 1$. An elegant solution for q based on the eigenvalue decomposition is referred to as the QUEST algorithm [10]. The problem may evoke the analogy with that of GPS multi-antenna attitude determination, but here we have to deal with incoherent sets of measurements: the magnetic field and the specific force. The concerned vectors are summarized in Table 2.

Table 2: The necessary vector observations for three-axis attitude determination using DMC and GPS.

	Body Frame (3-axis DMC)	Local-Level Frame (External reference)
Magnetic field (b)	$\mathbf{m}^b / \ \mathbf{m}^b\ $	$\mathbf{m}^l / \ \mathbf{m}^l\ $ - map
Specific force (f)	$\mathbf{f}^b / \ \mathbf{f}^b\ $	$\mathbf{f}^l / \ \mathbf{f}^l\ $ - see (9)

The first column of Table 2 denotes the normalized output of DMC magnetometers (m) and accelerometers (f) whose axis represent the body frame. The reference frame is chosen to be the local-level (l) geographical frame. The reference magnetic values are typically provided in this frame and can be usually considered constant over a small area (several km^2) and time period (months). The following relation holds for the second reference:

$$\mathbf{f}^l = \ddot{\mathbf{r}}^l + (2\boldsymbol{\Omega}_{ie}^l + \boldsymbol{\Omega}_{el}^l)\dot{\mathbf{r}}^l - \mathbf{g}^l \quad (9)$$

where $\ddot{\mathbf{r}}$ and $\dot{\mathbf{r}}$ are the acceleration and velocity vectors determined by GPS, respectively, and \mathbf{g} is the local gravity vector. The $\boldsymbol{\Omega}$ -terms are the skew-symmetric matrices representing the earth and local-level frame rotation that together with velocities define the Coriolis acceleration. In a static case, the equation (9) collapses to the value of local gravity reference \mathbf{g}^l that defines the horizontal plane for conventional applications of magnetometry.

The resulting attitude does not depend on the past measurements, as it is determined independently for each pair of vectors. Hence, neither the continuity of GPS measurements nor the initialization is the prerequisite. A singularity of this method could theoretically occur during a free fall along the local vertical ($\mathbf{f}^l = [0, 0, 0]$). This is, however, less likely to happen in the application considered.



Figure 6: The DMC (inset) and the GPS antenna are both mounted on skier's helmet. The azimuth derived by the former is related to direction of movement while the one of DMC/GPS is associated with the orientation of skier's body.

Preliminary testing

For the empirical tests we employed the DMC furnished by Vectronix [11] (inset of Figure 6). This sensor is designed to deliver azimuth and tilt information of 0.1 and 1-degree accuracies respectively in situations lacking local magnetic perturbation and kinematic accelerations. As the latter condition is violated in downhill skiing, the orientation calculated by the instrument cannot be directly used. Instead DMC's raw measurements (6-channels at 30Hz) are first low-passed filtered and then combined with GPS data as described in the previous section. The DMC and the L1/L2 GPS antenna were installed on the skier's helmet, while the GPS receiver and small data logger were kept in a waistband. The total weight of all instruments was about 0.5 kg.

Azimuth

The first tests lacked an independent source of attitude reference and therefore the obtained results can only be controlled indirectly.

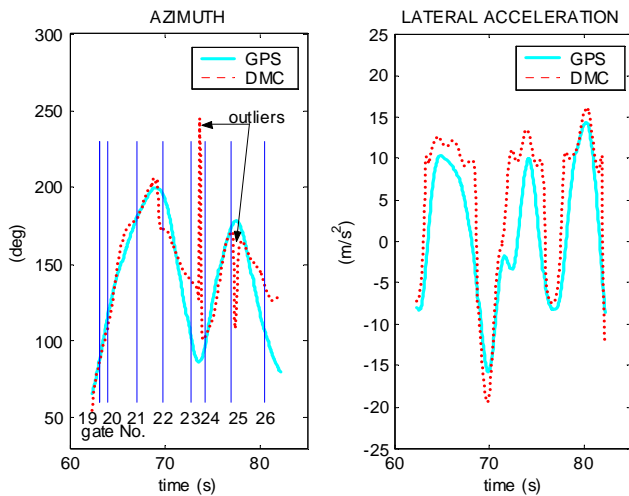


Figure 7: Comparison between azimuth and lateral accelerations obtained from GPS and DMC/GPS data.

Figure 7 shows two types of such assessment. First, the DMC azimuth is compared to the one obtained from the trajectory. Although the detected signals may differ due to the nature of skier's movement (see Figure 6 for explanation), both azimuths tend to align during straight-aways. While there are not many in modern downhill race, similar effect is achieved in zones with a gradual change of trajectory orientation, as it is the case between gates 19-24. As can be seen from Figure 7 there are some outliers in the DMC/GPS orientation. These are most likely caused by fast movements of the skier's head in the vertical direction over terrain jumps that may influence the geometric averaging of the magnetic field during the sensor's integration time. In this respect, gyro-stabilized magnetometers may be a better choice.

The second indirect comparison uses the derived 3D attitude matrix R to transform the measured specific force vector f^b from the body frame to the local-level frame f^l . Then, equation (9) is applied to estimate the kinematic accelerations and compare them to those derived by GPS. Again, the discrepancies in Figure 7 may indicate that the achieved orientation accuracy may be several degrees lower than what is expected in low dynamic.

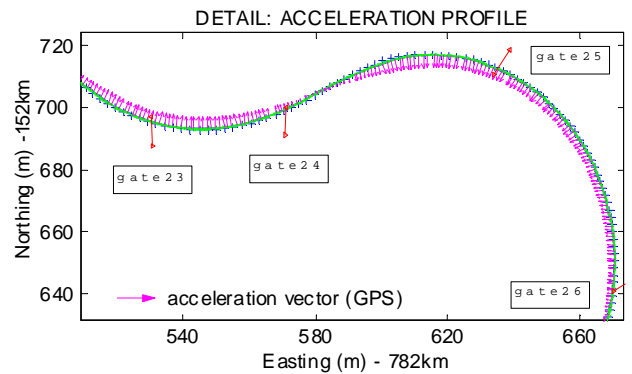


Figure 8: Coaches consider acceleration profile worth of analysis. This important trajectory parameter can be established by means of autonomous measurements.

Acceleration

As it has already been mentioned, coaches consider the acceleration profile a valuable indicator of racer's performance (Figure 8). To assess the DMC sensor quality in this respect without an influence of the attitude, the magnitude of the specific force vector was compared to that estimated by equation (9) using GPS data. The differences are at the order of 0.3 m/s^2 (1σ), which is few times higher than what is expected from the system specification. The sensitiveness of the accelerometer biases to the low temperatures is believed to be the cause. With the signal oscillating between $10\text{-}20 \text{ m/s}^2$, this accounts for sensor error of about 1.5-3%.

To supply a fully autonomous system (i.e. independent of GPS) that determines kinematic acceleration rather than the specific force (accelerometer output), an autonomous source of attitude needs to be put in place. As the accuracy

of currently available MEMS gyros is most likely insufficient for such a purpose, their synergy with magnetometers may offer an interesting alternative. In such a system the triaxial gyro output stabilizes the magnetometer reading and also provide the attitude autonomy over the periods when GPS signal is obstructed. On the other hand, DMC/GPS orientation gives the initial alignment that can be periodically repeated.

- The technique seems to be also appropriate for precise acceleration determination.
- A concept of attitude determination via the synergy of DMC/GPS was presented, although the questions related to the system accuracy could not be completely addressed. Further investigations are needed in this domain and the attention should be paid should be given to systems using gyro-stabilized magnetometer output.

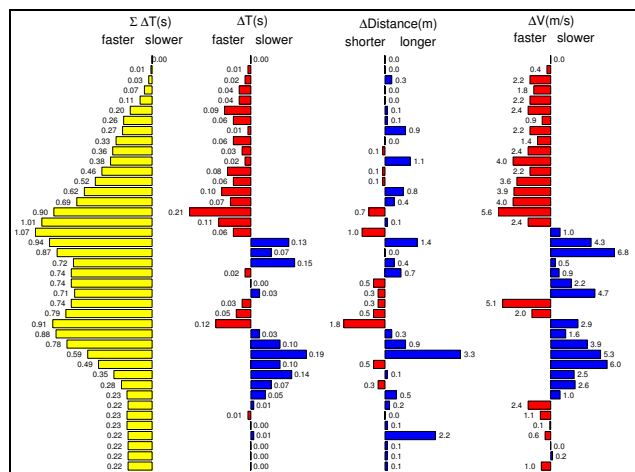


Figure 9: Performance comparison between two skiers at each gate. The first two columns from the left represent the accumulated time and gate-to-gate time differences, respectively. The third column shows the integrated distance along the fitted path, while the far-right column depicts the differences in instantaneous speed.

CONCLUSIONS

When answering a question like: “What was the exact trajectory of the downhill race winner and over which sections he gained/lost the precious few hundredths of a second?” we are facing an uneasy task of a surveyor that needs to deliver centimeter level precision at speeds of 120 km/h, 2g acceleration and quickly changing environmental conditions. We proposed a tactic to facilitate this assignment by a spatial filtering and investigated the use of MEMS sensors in deriving additional trajectory parameters. From these investigations the following conclusions can be drawn:

- The trajectory modeling by means of smoothing splines offers an elegant and practical tool to replace the discrete sampling with a set of continuous functions. The technique is appropriate to our application as the obtained model is continuous in second derivative and minimizes the acceleration profile. These aspects fit well the nature of athletes’ movement.
- The proposed method of filtering data with varying positioning accuracy proved to be effective with respect to the application.

The described methodology was applied during the Ski World Championship at St. Moritz in February 2003 where it held to the expectations. Precise trajectory analyses, like that presented in Figure 9 were furnished for men’s and women’s downhill. The obtained trajectories were also linked to the 3D terrain model and virtual-reality race was created for the broadcasters.

ACKNOWLEDGEMENT

This research was supported via a CTI grant attributed to the laboratories LCAV and TOPO at EPFL with the industrial support of Dartfish Corporation and Swiss TV. The support of DMC by Vectronix is greatly appreciated.

REFERENCES

1. Skalous, J., et al., *Athletic Analysis with Racing Hart*. GPS World, 2001: p. 14-18.
2. Skalous, J. and B. Merminod. *DGPS-Calibrated Accelerometric System for Dynamic Sports Events*. in *ION GPS*. 2000. Salt Lake City, Utah, USA.
3. Kleusberg, A. and P.J.G. Teunissen, *GPS for Geodesy*. 2nd ed. 1998: Springer.
4. O'Neill, B., *Elementary differential geometry*. 2 ed. 1997: Academic Press, cop.
5. de Boor, C., *A practical guide to splines*. Rev. ed. ed. Applied mathematical sciences. Vol. 27. 2001, New York: Springer-Verlag.
6. Dierckx, P., *Curve and Surface Fitting with Splines*. 1993, New York: Oxford University Press Inc.
7. Cannon, M.E., et al., *DGPS Kinematic Carrier Phase Signal Simulation Analysis for Precise Velocity and Position Determination*. NAVIGATION: Journal of The Institute of Navigation, 1997. **44**(2): p. 231-245.
8. Bruton, A.M., C.L. Glennie, and K.P. Schwarz, *Differentiation for High Precision GPS Velocity and Acceleration Determination*. GPS Solutions, 1999. **2**(4): p. 7-22.
9. Wahba, G., *A Least Squares Estimate of Spacecraft Attitude*. SIAM Review, 1965. **7**(3): p. 409.
10. Schuster, M.D. and S.D. Oh, *Three-Axis Attitude Determination from Vector Observations*. Guidance and Control, 1981. **4**(1): p. 70-77.
11. Vectronix, *DMC-SX*. 2000, Heerbrougg, Switzerland.